

RSC Advances



This is an *Accepted Manuscript*, which has been through the Royal Society of Chemistry peer review process and has been accepted for publication.

Accepted Manuscripts are published online shortly after acceptance, before technical editing, formatting and proof reading. Using this free service, authors can make their results available to the community, in citable form, before we publish the edited article. This *Accepted Manuscript* will be replaced by the edited, formatted and paginated article as soon as this is available.

You can find more information about *Accepted Manuscripts* in the [Information for Authors](#).

Please note that technical editing may introduce minor changes to the text and/or graphics, which may alter content. The journal's standard [Terms & Conditions](#) and the [Ethical guidelines](#) still apply. In no event shall the Royal Society of Chemistry be held responsible for any errors or omissions in this *Accepted Manuscript* or any consequences arising from the use of any information it contains.

**Enhancing insulation of wide-range spectrum in the PVA/N thin film by
doping ZnO nanowires**

Yu-Chen Lin,¹ Ching-Hsiang Chen,² Liang-Yih Chen,³ Shih-Chieh Hsu,^{4,5,*} and Shizhi Qian⁶

¹Department of Photovoltaic Materials Equipment, Precision Machinery Research &
Development Center, 569, Sec II, Po-Ai Rd., Chiayi City 60060, Taiwan

²Graduate Institute of Applied Science and Technology, National Taiwan University of Science
& Technology, Taipei, Taiwan

³Department of Chemical Engineering, National Taiwan University of Science and Technology,
43, Section 4, Keelung Road, Taipei, 106, Taiwan

⁴Department of Chemical and Materials Engineering, Tamkang University, Tamshui, New
Taipei City, 25137, Taiwan

⁵Energy and Opto-Electronic Materials Research Center, Tamkang University, Tamshui, New
Taipei City, 25137, Taiwan

⁶Institute of Micro/Nanotechnology, Old Dominion University, Norfolk, VA 23529, USA

*Corresponding author: Tel:+886-26215656ext2032; Fax:+886-26209887; E-mail:
roysos@mail.tku.edu.tw (Shih-Chieh Hsu)

Abstract

In this study, polyvinyl alcohol/nitrogen (PVA/N) hybrid thin films doped sharp-sword ZnO nanowires possessing the insulating effect with wide-range spectrum is demonstrated for the first time. PVA/N doped ZnO nanocomposites were developed by blending PVA and N-doped ZnO nanowires in water at room temperature. Measurements from the field emission scanning electron microscopy (FE-SEM), X-ray diffraction (XRD), Raman, and Photoluminescence emission (PL) spectra of the products show that nitrogen is successfully doped into the ZnO wurtzite crystal lattice. In addition, the refractive index of PVA/N doped ZnO hybrid thin films can be controlled by varying the doped ZnO nanowires under different NH_3 concentrations. It is believed that PVA/N doped ZnO hybrid thin films provide a suitable candidate for further emerging applications like heat-shielding coatings on smart windows.

Keywords: Polymer-Matrix Composites (PMCs), PVA/N Doped ZnO, Nanocomposites, Heat Shielding

1. Introduction

Polymer matrix nanocomposites with inorganic nanofiller, particularly with metal oxides, have drawn significant attention for their potential applications in optical products due to their unique optical, electrical, and mechanical properties¹⁻³. Polymer matrixes and metal oxides can be synthesized together as novel materials used in many potential applications^{4,5}. For example, in the smart window application, the heat shielding films are able to control the sunlight energy spectrum because the visible light needs to be transmitted, and near-infrared should be cut for thermal insulation, producing the energy-saved effect. Recently, the coatings with low emissivity heat shielding also attract significant attention because polymer nanocomposites with metal oxide nanofiller can modify the optical, thermal, and mechanical properties⁶⁻⁸.

Polyvinyl alcohol (PVA) has several advantages such as easy synthesis, non-toxicity, water-solubility, transparency, good environmental stability, thermal stability, and film-forming ability⁹. It is also a promising material for the development of optical technological, pharmaceutical, biomedical and membrane applications¹⁰. Furthermore, polymer/metal oxide nanocomposites can be formed via the hydrogen bonding between the –OH groups of PVA and the functional groups of metal oxides¹¹.

Among all metal oxide materials, zinc oxide (ZnO) is a n-type semiconductor material with wide band gap ($E_g = 3.34$ eV), although this definition is still under debate¹². It has high exciton binding energy (60 meV) and attracted a lot of interest over the past decade due to the presence of native defects related to oxygen vacancies and shallow zinc interstitials, both of which act as donors¹³⁻¹⁶. Some investigations report that ZnO can not only act as donors, but also acceptors^{17,18}. It also shows some beneficial properties, including good transparency, high electron mobility, and strong luminescence¹³⁻¹⁶. Therefore, ZnO is typically adopted as

transparent films in several emerging applications, including the smart window of energy-saving and heat shielding, thin-film transistors, light-emitting diodes¹⁹⁻²¹, solar cells^{22,23}, and biomedical applications²⁴, etc. To further improve its performance in optoelectronic applications, ZnO based nanomaterials have been developed by doping group I and V elements²⁵⁻³². Many experimental results show that substituting O sites of ZnO is capable of modulating its electrical and optical properties. Among various dopant elements, nitrogen is the most promising candidate because of its smallest ionization energy and its atomic radius which is similar to the one of oxygen^{33,34}.

The optical properties of pure PVA polymer films show no remarkable absorption bands in the range of UV-Vis and generate photo degradation easily when they are exposed in UV light³⁵. Several methods have been applied by combining ZnO derivatives with the PVA during film-forming. For example, Augustine et al.⁶ introduced oleic acid containing groups onto the surfaces of ZnO nanorods embedded in PVA matrix to prepare the highly transparent nanocomposite films. Moreover, Tan et al.³⁶ reported that the performance of PVA/ZnO nanorods redox sensors is enhanced due to the property of the ZnO, which effectively facilitates the electron transfer and provides better stability and stronger signal. Subsequently, Roy et al.³⁷ reported the relaxation, electronic transportation, and conduction mechanism of PVA/ZnO nanocomposites by a solution casting technique which is influenced by the applied frequencies. However, these studies³⁵⁻³⁷ pointed out that the PVA/N thin films doped ZnO were able to insulate UV light only. The limitation of light insulation hinders the applications in the wide use of heat shielding materials. Here, the “Optical insulation” is defined as an ability to partially block the light from UV to IR. Since the PVA/N doped ZnO thin film can effectively keep off the sun light outside, it also has the function of heat insulation. The combined features of optical

and heat insulations enable the hybrid film to become a suitable candidate for energy-saving applications such as heat-shielding coatings on smart windows.

In order to insulate wide-range spectrum, we propose a simple and effective method to prepare PVA hybrid thin films with sharp-sword ZnO nanocomposites by controlling N species in the ZnO nanowires. We found that doping N into the whole system to form the sharp-sword ZnO nanowires can insulate the wide-range spectrum, especially the IR light, because there are defects in the ZnO nanowires. Our technique of PVA/N doped with sharp-sword ZnO nanowires is capable of insulating the wide-range spectrum instead of only the UV spectrum reported in the existing studies. The structure, morphology, and optical properties of N-doped ZnO nanowires will be characterized by using XRD, PL, and Raman scattering. The correlations between the experimental conditions and the performance of the PVA/N doped ZnO hybrid thin films will be investigated and discussed in detail by the spectroscopic technique.

2. Experimental

2.1. Materials

Poly (vinyl alcohol) (PVA, 98–99% hydrolyzed, MW 13,000–23,000) and Polyethyleneimine (PEI, MW 800) were purchased from Aldrich. Zinc acetate dehydrate ($\text{Zn}(\text{OAc})_2 \cdot 2\text{H}_2\text{O}$) and hexamethylenetetramine [$(\text{CH}_2)_6\text{N}_4$] were purchased from Merck. Indium tin oxide (ITO) glass substrates, whose content is $\text{Sn}_2\text{O}_3:\text{In}_2\text{O}_3=1:9$, were purchased from Lumtec. Deionized (DI) water with resistivity of 1 $\text{M}\Omega\text{-cm}$ was prepared by deionized water machine (model: RDI-20) produced by Lotuntech.

2.2. Preparation of the N-doped ZnO nanowires

The N-doped ZnO nanowires were synthesized by the hydrothermal method. First, $\text{Zn}(\text{OAc})_2 \cdot 2\text{H}_2\text{O}$ (25 mM), $(\text{CH}_2)_6\text{N}_4$ (25 mM) and PEI molecules (5 mM) were dissolved individually in DI water to form a 40 mL solution. ITO glass substrates were immersed into the detergent, DI-water, ethanol, and 1-propanol in order and washed by ultrasonic bath. After washing, the ITO glass substrates were blown by N_2 gas for dry. We stirred the mixture at room temperature for 1 hr to form a homogeneous solution and then placed it into the Teflon-lined steel autoclave for 90°C for 24 hrs. The line-type growth began to form ZnO nanowires onto the ITO substrate. After growth process, the samples were rinsed with DI water to remove any residual salt or amino complex. Subsequently, the samples were dried under vacuum for 12 hrs at 60°C to obtain the pristine ZnO (referring to sample S1). Finally, the samples were annealed at 400°C for 2 hrs in ambient air. We obtained the doped samples of S2 and S3 by using NH_3 to adjust the solution pH to 9 and 11, respectively.

2.3. Preparation of the PVA/N doped ZnO thin film

The PVA/N doped ZnO nanocomposite was prepared by ultrasonically dispersing the N-doped ZnO nanowires into the PVA solution (PVA/N doped ZnO: 1000mg/20mg, DI water:15 mL), and the mixture was stirred and heated at 100°C for 1 hr. Then we used the spin-coating technique to form a PVA/N doped ZnO thin film, which have 2 wt% of N-doped ZnO nanowires. The thickness of the films was controlled by the coating times (5 layers) and the speed of the spin-coating unit (3,000 rpm). Finally, the films, labeled as PVA, PVA/S1, PVA/S2, and PVA/S3, were heated to 40°C for 10 min.

2.4. Equipments and measurements

The morphology was analyzed by field emission scanning electron microscopy of Hitachi S-5000 system (Hitachi, Japan). X-ray diffraction patterns were characterized by a Rigaku X-ray

diffractometer (model-D/Max-2B, $\text{CuK}\alpha$ radiation at a scanning rate of 1° min^{-1} from 20° – 75° , 30 kV). The RAMaker system (Protrustech Corporation Limited), which can measure 532 nm diode pumped solid state (DPSS) laser excited Raman spectra and 325 nm He-Cd laser PL spectra, is equipped with one Andor iDus TE cooled CCD of 1024×128 pixels. The ellipsometry data was collected by Elli-SE (Ellipso Technology Company) to obtain the n and k values of the PVA/N doped ZnO nanocomposite on glass films.

3. Results and discussion

In Fig. 1, the morphologies of the as-grown pristine ZnO and N-doped ZnO nanowires were observed by FE-SEM. As shown in Fig. 1a, the pristine ZnO nanowires (S1) shape like irregular columns and their diameters are approximately 300-400 nm. However, the diameter of the N-doped ZnO nanowires (S2) was about 100-200 nm with the length of about 2 μm . The N-doped ZnO nanowires (S2) possess high density and grow along the axis evenly. The results indicated that NH_3 could restrain lateral growth of ZnO (Fig. 1b)⁴⁴. When pH is increased to 11, the N-doped ZnO nanowires will shape sharp-pointedly with the diameters of 400-900 nm (Fig. 1c). Those morphologies were similar to those observed on the as-grown phosphorus-doped p-type ZnO nanowires by the hydrothermal method²⁶.

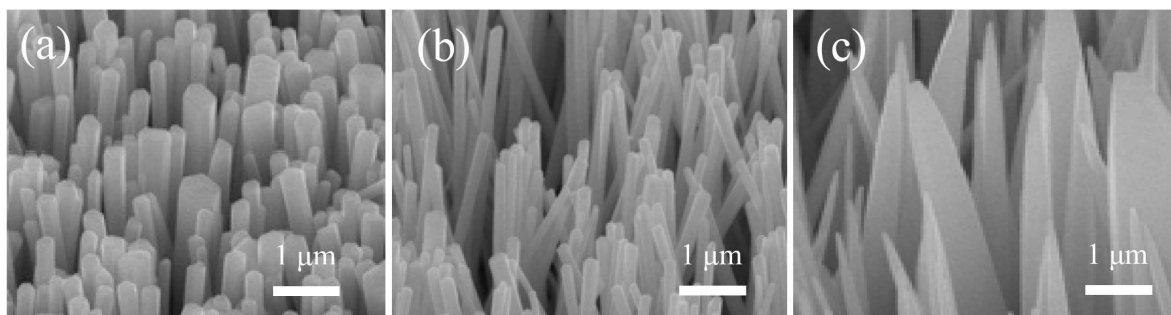


Fig. 1. FE-SEM images of the pristine ZnO and N-doped ZnO nanowires prepared in (a) S1, (b) S2, and (c) S3.

The properties of the nitrogen doped into ZnO crystal lattices prepared by the hydrothermal method are further investigated. The XRD measurements of the pristine ZnO and N-doped ZnO nanowires prepared under the alkaline environment are shown in Fig. 2. The magnification of the (002) diffraction peaks were observed (inset in Fig. 2). The diffraction peak of 34.4° observed in the pristine ZnO (S1) can be attributed to the ZnO wurtzite crystal structure, which is a preferential crystal orientation along the c -axis (Fig. 2a)^{26,38}. In the XRD spectrum of N-doped ZnO nanowires (S2 and S3), diffraction still peaks at 34.4° (Fig. 2b-c). For S1, S2 and S3, the full-width at half maximum (FWHM) of the (002) diffraction peak were 0.31° , 0.33° , and 0.40° , respectively. These results reveal that the crystallinity of ZnO nanowires slightly decreased with the doped N ions. This may be due to the fact that the preferential adsorption of NH_3 on crystal lattice causes the N ions to substitute the Zn sites to form complex defects^{26,38,39}, the situation of which is similar to the Ag-N doped p type ZnO films prepared by sol-gel method⁴⁰.

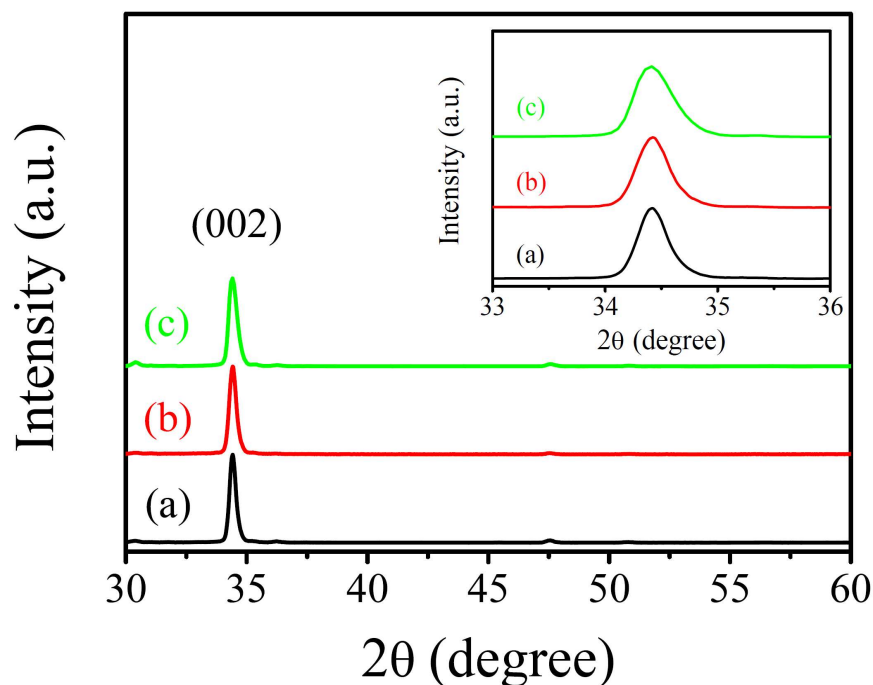


Fig. 2. XRD spectra of the pristine ZnO and N doped ZnO nanowires prepared in (a) S1, (b) S2, and (c) S3. Inset: the magnification of the (002) diffractive peaks

Fig. 3 depicts the Raman spectra of the samples S1, S2, and S3. There are wurtzite ZnO structures in the undoped ZnO nanowires, including 332, 383, 438, 584 and 1158 cm^{-1} . The corresponding models of molecular movement are 2- E_2 (M), A_1 (TO), E_2 (high frequency), E_1 (LO) modes, and C–O bonds⁴¹⁻⁴⁴. In the Raman spectrum of S2, the spectral peaks at approximately 278, 511, 584 and 645 cm^{-1} were observed (Fig. 3b). Those peaks indicate that several modes were formed due to the nitrogen-related local vibrational modes of the N-doped ZnO by the NH_3 treatment⁴⁴⁻⁴⁷. When the pH value of solution increases, the spectral peaks of the S3 become more obvious than those of the samples S1 and S2 (Fig. 3c). This finding might be ascribed to the increase of nitrogen content in N-doped ZnO nanowires, which formed the defects by N incorporation. The results were consistent with the XRD analysis (Fig. 2) and similar to the stable *p*-type ZnO film, which was fabricated by radio frequency sputter deposition and ion beam sputter deposition, on Si and quartz glass substrates by nitrogen doping^{48,49}.

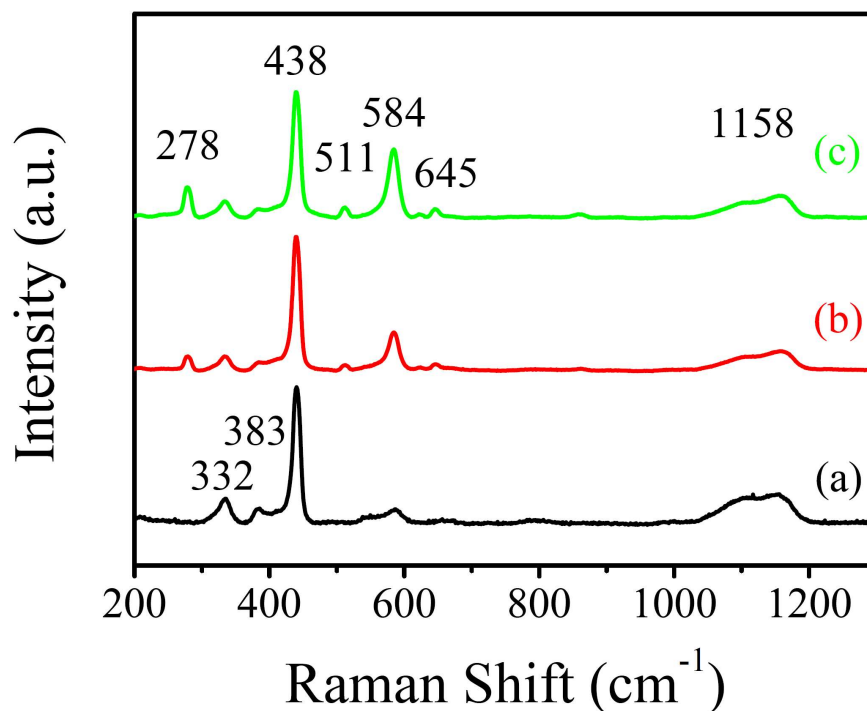


Fig. 3. Raman spectra of the pristine ZnO and N-doped ZnO nanowires prepared in (a) S1, (b) S2, and (c) S3

Fig. 4 shows the PL spectra, excited by the 325 nm He-Cd laser, of the pristine ZnO and N-doped ZnO nanowires in various pH values at room temperature. The peak of ultraviolet emission at about 382 nm of the pristine ZnO nanowires could be identified. The peak appears because the near band-edge excitonic emission (NBE) of ZnO is generated by the recombination of the free excitons via an exciton collision process (inset in Fig. 4a)^{26,50-52}. So far as the N-doped ZnO nanowire is concerned, the near band-edge emission will lead to a blue-shift from 382 to 379 nm. If we increase the pH value to produce the N-doped ZnO, the emission intensity of the ultraviolet area will decrease (Inset in Fig. 4b and c). These results indicated that the shift of the peak in the UV region tends toward high energy probably because the O sites are replaced by N in the ZnO crystal lattices^{26,52,53}.

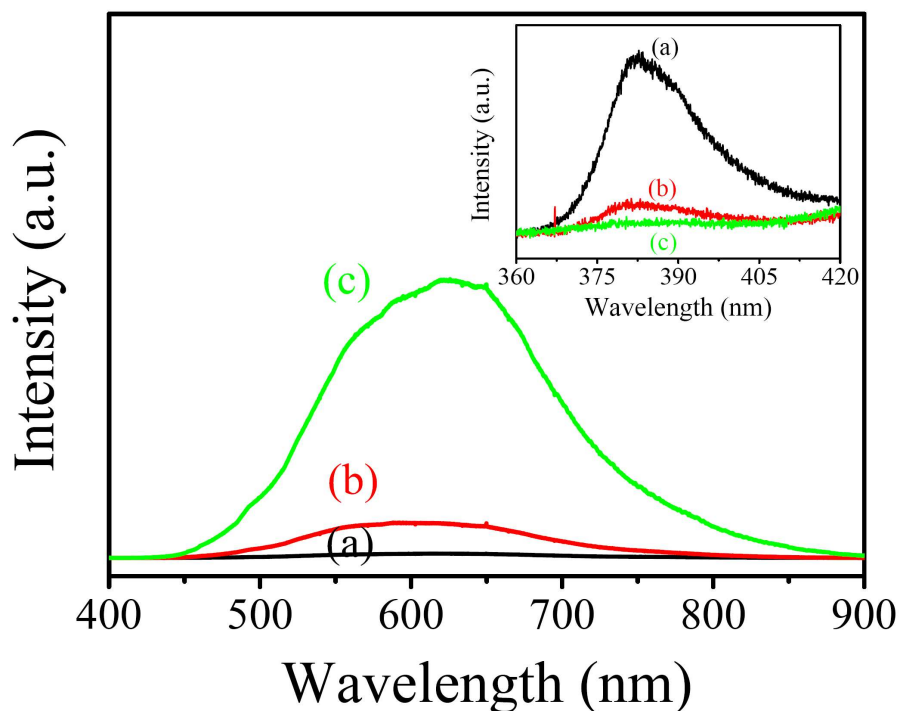


Fig. 4. PL spectrum of the pristine ZnO and N-doped ZnO nanowires prepared in (a) S1, (b) S2, and (c) S3. Inset: the magnification of the ultraviolet emission region.

In addition, the intensity of visible emission related to the defects in the pristine ZnO nanowires was weak (Fig. 4a). The intensity of orange emission of N-doped ZnO nanowires at about 607 and 624 nm become stronger with the increase of pH values (Fig. 4b and c). The orange emission is related to the intrinsic defects which are formed with N incorporated with the ZnO, such as oxygen vacancy or zinc intrinsic^{26,52-55}. The behavior is consistent with the analyses of XRD and Raman spectra. The wavelength of PL emission is observed to be higher in the region of orange emission than the results reported in the literature^{4,13}, in which Cu is doped into ZnO nanoparticle sheets prepared by a solution route at low temperature. These results indicate that Cu doping in the ZnO crystal lattices induces yellow emission because of the oxygen interstitials or the zinc vacancies. The yellow emission shows gradual blue-shifts with the increase of Cu concentrations in the ZnO⁵⁶. However, in our systems, it might arise from the

shapes of N-doped ZnO nanowires or the N occupying in the ZnO crystal lattices, which were similar to the phosphorus-doped ZnO nanorods by the hydrothermal method²⁶. These results are attributed to the P doping in the ZnO crystal lattices. In addition, the N atom is smaller than the P and Cu atoms, thus it will cause the visible emission produced by the defect in the crystal of the N-doped ZnO nanowires to have a red-shift.

The refractive dispersion plays an important role in optical materials. In order to calculate the optical constant refractive index (n) and extinction coefficient (k) of the films at different wavelengths, we applied the following equations^{27,57}:

$$\alpha = (1/d) \ln[(1 - R)^2 / 2T] + (1 - R)^2 / (4T^2 + R^2)^{1/2}, \quad (1)$$

$$n = [(R + 1) / (R - 1)] + \{[(R + 1) / (R - 1)]^2 - (1 - k^2)\}^{1/2}, \quad (2)$$

and

$$k = \alpha\lambda/4\pi. \quad (3)$$

In the above, α is the absorption coefficient, d is the film thickness, R is the reflectance, T is the transmittance, and λ is the wavelength. According to the equation (3), k is related to α and λ . The n and k of PVA, PVA/pristine ZnO (S1) and PVA/N doped ZnO (S2, S3) hybrid films as a function of the wavelength are shown, respectively, in Figs. 5a and 5b. For PVA film, the intensity of n remains weak with the increase in the wavelength. Value of n for PVA/S1 film slightly increased with an increase in wavelength. Comparing it with the hybrid films of PVA/S2 and PVA/S3, we find that in the visible and the near-infrared regions, the value of n increases with an increase in the wavelength. The above results can also correspond to the measurement of k value. The phenomenon also indicates low light scattering and high absorbance²⁷. The increase of the refractive index is attributed to higher density and lower surface roughness of the stacked films with the N-doped ZnO in the PVA matrix (PVA/S2 and PVA/S3)⁵⁸ when compared to

refractive index of the PVA/S1 films. We can attribute the result to the decline of volume fraction of the voids on the surface of the PVA hybrid films. This outcome is different from the Na-doped ZnO thin films⁵⁹ and the Cu-doped ZnO films⁶⁰. The results also indicate that the N dopant changes the structural and optical properties of the PVA/N doped ZnO hybrid films. Therefore, we can control the refractive index of the PVA/N doped ZnO hybrid nanocomposite films by varying the composition with N-doped ZnO nanowire, which is important for the applications in designing the window products.

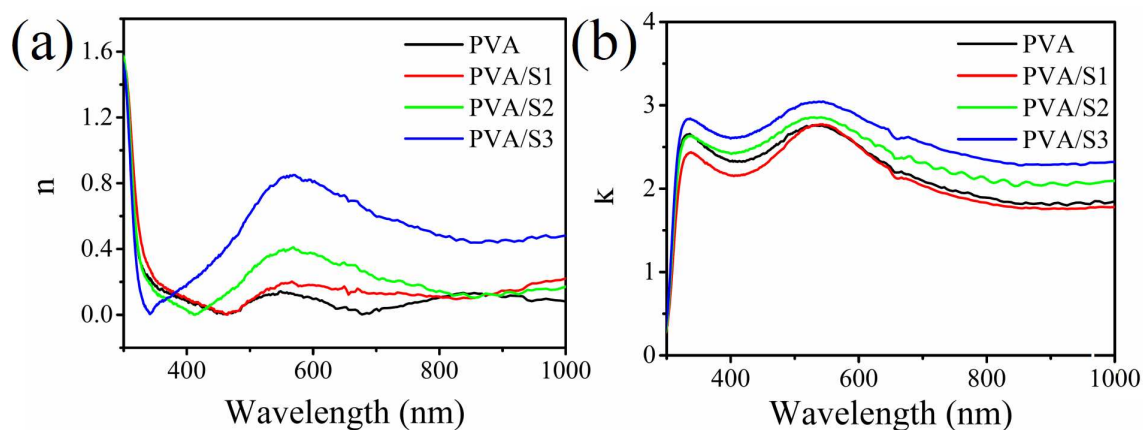


Fig. 5. (a) Refractive indices and (b) extinction coefficients spectrum for the PVA, PVA/pristine ZnO and PVA/N doped ZnO hybrid nanocomposite films.

The surface and cross-sectional morphologies of the PVA/N doped ZnO hybrid films coated on the glass substrates were investigated by FE-SEM. The PVA/N doped ZnO hybrid films exhibited a homogeneous surface (Fig. 6a), the results are consistent with the n , k results. In addition, the cross-section morphology of the PVA/N doped ZnO hybrid films shows a dense microstructure by stacking between the N-doped ZnO nanowires and PVA matrix, and the thickness of the film was about 300 nm (Fig. 6b). In Fig. 6, we observed that unlike the PVA/N hybrid thin film with ZnO particles, which will produce space while they are stacked, the PVA/N

doped ZnO hybrid thin film has rather condensed structure, which can improve the properties of the polymer owing to its even dispersion in the matrix.

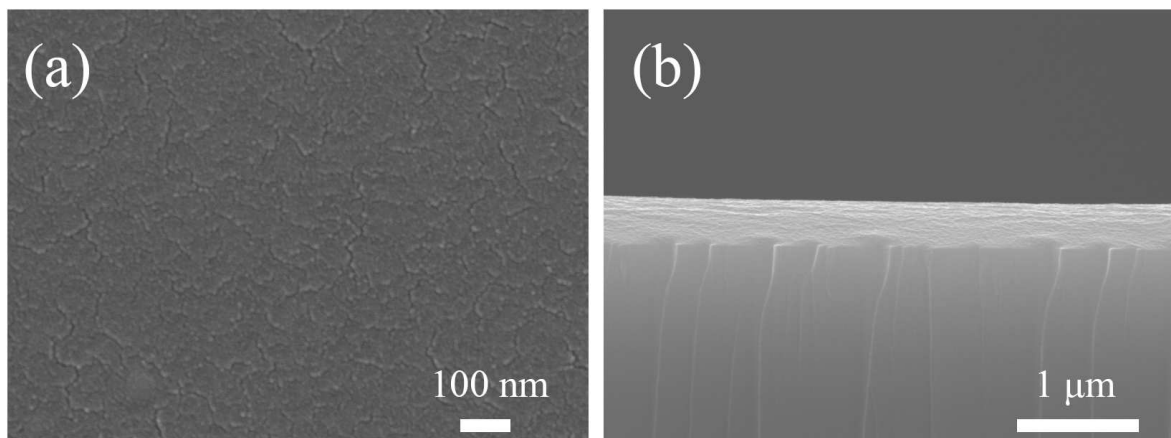


Fig. 6. FE-SEM images of the PVA/N doped ZnO (S3) thin films prepared (a) planar and (b) cross-section.

4. Conclusions

PVA hybrid thin films with N-doped ZnO nanowires were successfully synthesized by the hydrothermal method in NH_3 . Measurements of refractive indices and extinction coefficients spectrum showed that the prepared film is capable of insulating the wide-range spectrum from UV to IR for the first time. This wide-range insulating spectrum effect can be attributed to the sharp-sword ZnO nanowires which formed by the adsorption of NH_3 on the ZnO crystal lattice. The refractive index of PVA/N doped ZnO hybrid thin films can be controlled by doping various amounts of N in the ZnO nanowires under different NH_3 concentrations. Measurements of the XRD, Raman, and PL spectra proved that the nitrogen was doped into the ZnO wurtzite crystal lattice and substituted for O site to form complex defects. The SEM images also showed that PVA/N doped ZnO hybrid thin films have rather condensed structure and homogeneous surface.

This approach is expected to be a great contribution to enhance the range of insulating wavelength of the PVA hybrid thin film by well-controlling N-doped ZnO nanowires. The result is crucial for the applications of designing effective products of solar heat shielding.

Acknowledgements

This work was financially supported by the Ministry of Science and Technology of the Republic of China (Taiwan) under Grant 101-2623-E-032-002-ET, 102-2623-E-032-001-ET and the Ministry of Economic Affairs of the Republic of China under Grant 102-EC-17-A-02-02-0756.

References

- 1 M. Abdullah, T. Morimoto, K. Okuyama, *Adv. Funct. Mater.*, 13, 2003, 800
- 2 N. Dal'Acqua, F.R. Scheffer, R. Boniatti, B.V.M. da Silva, J.V. de Melo, J. da Silva Crespo, M. Giovanela, M.B. Pereira, D.E. Weibel, G. Machado, *J. Phys. Chem., C* 117, 2013, 23235
- 3 Y.D. Liu, X. Quan, B. Hwang, Y.K. Kwon, H.J. Choi, *Langmuir*, 30, 2014, 1729
- 4 M.-Y. Hua, Y.-C. Lin, R.-Y. Tsai, H.-C. Chen, Y.-C. Liu, *Electrochim. Acta*, 56, 2011, 9488
- 5 L.Y. Ng, A.W. Mohammad, C.P. Leo, N. Hilal, *Desalination*, 308, 2013, 15
- 6 M. Sajimol Augustine, P.P. Jeeju, V.G. Sreevalsa, S. Jayalekshmi, *J. Phys. Chem. Solids*, 73 2012, 396
- 7 J. Lee, D. Bhattacharyya, A.J. Easteal, J.B. Metson, *Curr. Appl. Phys.*, 8, 2008, 42
- 8 X.M. Sui, C.L. Shao, Y.C. Liu, *Appl. Phys. Lett.*, 87, 2005, 113115
- 9 S. Majumdar, B. Adhikari, *Sens. Actuators B: Chem.*, 114, 2006, 747
- 10 Y. Tan, Y. Song, Q. Zheng, *Nanoscale*, 4, 2012, 6997
- 11 H.N. Chandrakala, B. Ramaraj, Shivakumaraiah, J.H. Lee, Siddaramaiah, *J. Alloys Compd.*, 580, 2013, 392
- 12 A. Janotti, Chris G Van de Walle, *Rep. Prog. Phys.*, 72, 2009, 126501
- 13 R.M. Nyffenegger, B. Craft, M. Shaaban, S. Gorer, G. Erley, R.M. Penner, *Chem. Mater.*, 10,

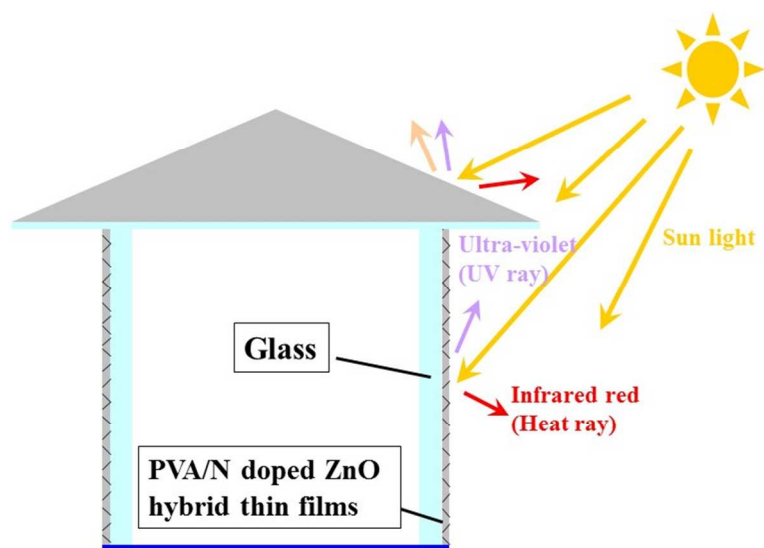
1998, 1120

- 14 L. Irimpan, V.P.N. Nampoory, P. Radhakrishnan, *J. Appl. Phys.*, 103, 2008, 094914
- 15 D.W. Hatchett, M. Josowicz, *Chem. Rev.*, 108, 2008, 746
- 16 S.B. Zhang, S.H. Wei, A. Zunger, *Phys. Rev.*, B 63, 2001, 075205
- 17 J. Han, F. Fan, C. Xu, S. Lin, M. Wei, X. Duan, Z.-L. Wang, *Nanotechnology*, 21, 2010, 405203
- 18 R. T. Ginting, C. C. Yap, M. Yahaya, M. M. Salleh, *ACS Appl. Mater. Interfaces*, 6, 2014, 5308
- 19 C.-H. Chen, S.-J. Chang, S.-P. Chang, M.-J. Li, I.C. Chen, T.-J. Hsueh, A.-D. Hsu, C.-L. Hsu, *J. Phys. Chem.*, C 114, 2010, 12422
- 20 S.-J. Lim, J.-M. Kim, D. Kim, S. Kwon, J.-S. Park, H. Kim, *J. Electrochem. Soc.*, 157, 2010, H214
- 21 O. Lupan, T. Pauporté, B. Viana, I.M. Tiginyanu, V.V. Ursaki, R. Cortès, *ACS Appl. Mater. Interfaces*, 2, 2010, 2083
- 22 J. A. Anta, E. Guillén, and R. Tena-Zaera, *J. Phys. Chem.*, C 116, 2012, 11413
- 23 Y. Xie, P. Joshi, S.B. Darling, Q. Chen, T. Zhang, D. Galipeau, and Q. Qiao, *J. Phys. Chem.*, C 114, 2010, 17880
- 24 Y. Zhang, T.R. Nayak, H. Hong, W. Cai, *Curr Mol Med*, 13, 2013, 1633
- 25 B. Sieber, H. Liu, G. Piret, J. Laureyns, P. Roussel, B. Gelloz, S. Szunerits, R. Boukherroub, *J. Phys. Chem.*, C 113, 2009, 13643
- 26 X. Fang, J. Li, D. Zhao, D. Shen, B. Li, X. Wang, *J. Phys. Chem.*, C 113, 2009, 21208
- 27 M. Mazilu, N. Tigau, V. Musat, *Opt. Mater.*, 34, 2012, 1833
- 28 X. Yan, T. Itoh, S. Dai, Y. Ozaki, Y. Fang, *J. Phys. Chem. Solids*, 74, 2013, 1127
- 29 Y. Li, X. Zhao, W. Fan, *J. Phys. Chem.*, C 115, 2011, 3552
- 30 T.P. Rao, M.S. Kumar, *J. Alloys Compd.*, 506, 2010, 788
- 31 P.K. Ooi, S.S. Ng, M.J. Abdullah, Z. Hassan, *Mater. Lett.*, 116, 2014, 396
- 32 H. Wang, R. Bhattacharjee, I.M. Hung, L. Li, R. Zeng, *Electrochim. Acta*, 111, 2013, 797
- 33 C.H. Park, S.B. Zhang, S.-H. Wei, *Phys. Rev.*, B 66, 2002, 073202
- 34 R. Asahi, T. Morikawa, T. Ohwaki, K. Aoki, Y. Taga, *Science*, 293, 2001, 269
- 35 D.M. Fernandes, A.A.W. Hechenleitner, S.M. Lima, L.H.C. Andrade, A.R.L. Caires, E.A.G. Pineda, *Mater. Chem. Phys.*, 128, 2011, 371

- 36 S. Tan, X. Tan, J. Jiang, J. Xu, J. Zhang, D. Zhao, L. Liu, Z. Huang, *J. Electroanal. Chem.*, 668, 2012, 113
- 37 A.S. Roy, S. Gupta, S. Sindhu, A. Parveen, P.C. Ramamurthy, *Composites: Part B*, 47, 2013, 314
- 38 H. Qin, W. Li, Y. Xia, T. He, *ACS Appl. Mater. Interfaces*, 3, 2011, 3152
- 39 D.G. Cahen, Jean-Marc; Schmitz, Claus; Chernyak, Leonid; Gartsman, Konstantin; Jakubowicz, Abram, *Science*, 258, 1992, 271
- 40 L. Duan, W. Zhang, X. Yu, P. Wang, Z. Jiang, L. Luan, Y. Chen, D. Li, *Solid State Commun.*, 157, 2013, 45
- 41 W.-W. Zhong, F.-M. Liu, L.-G. Cai, X.-Q. Liu, Y. Li, *Appl. Surf. Sci.*, 257, 2011, 9318
- 42 K.A. Alim, V.A. Fonoberov, A.A. Balandin, *Appl. Phys. Lett.*, 86, 2005, 053103
- 43 B.M. Keyes, L.M. Gedvilas, X. Li, T.J. Coutts, *J. Cryst. Growth*, 281, 2005, 297
- 44 N.P. Herring, L.S. Panchakarla, M.S. El-Shall, *Langmuir*, 30, 2014, 2230
- 45 Z.W. Dong, C.F. Zhang, H. Deng, G.J. You, S.X. Qian, *Mater. Chem. Phys.*, 99, 2006, 160
- 46 J. Karamdel, C.F. Dee, B.Y. Majlis, *Appl. Surf. Sci.*, 256, 2010, 6164
- 47 A. Kaschner, U. Haboek, M. Strassburg, M. Strassburg, G. Kaczmarczyk, A. Hoffmann, C. Thomsen, A. Zeuner, H.R. Alves, D.M. Hofmann, B.K. Meyer, *Appl. Phys. Lett.*, 80, 2002, 1909
- 48 S. Dhara, P.K. Giri, *Thin Solid Films*, 520, 2012, 5000
- 49 L.-C. Chao, J.-W. Chen, H.-C. Peng, C.-H. Ho, *Surf. Coat. Technol.*, 231, 2013, 492
- 50 P.K. Samanta, P.R. Chaudhuri, *Sci. Adv. Mater.* 3, 2011, 107
- 51 A. Umar, B. Karunagaran, E. Suh, Y. Hahn, *Nanotechnology*, 17, 2006, 4072
- 52 J.-F. Chien, C.-H. Chen, J.-J. Shyue, M.-J. Chen, *ACS Applied Materials interfaces*, 4, 2012, 3471
- 53 D.Y. Lee, J.-E. Cho, N.-I. Cho, M.-H. Lee, S.-J. Lee, B.-Y. Kim, *Thin Solid Films*, 517, 2008, 1262
- 54 J.W. Chiou, K.P.K. Kumar, J.C. Jan, H.M. Tsai, C.W. Bao, W.F. Pong, F.Z. Chien, M.-H. Tsai, I.-H. Hong, R. Klauser, J.F. Lee, J.J. Wu, S.C. Liu, *Appl. Phys. Lett.*, 85, 2004, 3220
- 55 Q. Zhao, X.Y. Xu, X.F. Song, X.Z. Zhang, D.P. Yu, C.P. Li, L. Guo, *Appl. Phys. Lett.*, 88, 2006, 033102
- 56 R.-C. Wang, H.-Y. Lin, *Mater. Chem. Phys.*, 125, 2011, 263

- 57 S.Z. Ilican, Muhsin; Caglar, Yasemin; Caglar, Mujdat, *Opt. Appl.*, 36, 2006, 29
- 58 Y. Okuhara, T. Kato, H. Matsubara, N. Isu, M. Takata, *Thin Solid Films*, 519, 2011, 2280
- 59 J. Lv, K. Huang, X. Chen, J. Zhu, C. Cao, X. Song, Z. Sun, *Opt. Commun.*, 284, 2011, 2905
- 60 M. Caglar, F. Yakuphanoglu, *Appl. Surf. Sci.*, 258, 2012, 3039

Graphic abstract



PVA/N doped ZnO hybrid thin films provide a protection against harmful UV and IR rays.